Pathways through an Eclectic Universe
ASP Conference Series, Vol. 390, © 2008
J. H. Knapen, T. J. Mahoney, and A. Vazdekis, eds.

Circumnuclear Regions of Star Formation in Early-type Galaxies

Ángeles I. Díaz,[1] Elena Terlevich,[2] Guillermo F. Hägele,[1] and Marcelo Castellanos[1]

[1]*Departamento de Física Teórica, Universidad Autónoma de Madrid, Spain*
[2]*Instituto Nacional de Astrofísica, Óptica y Electrónica, Puebla, Mexico*

Abstract. Circumnuclear star-forming regions, also called hotspots, are often found in the inner regions of some spiral galaxies where intense processes of star formation are taking place. In the UV, massive stars dominate the observed circumnuclear emission, even in the presence of an active nucleus, contributing between 30 and 50% to the total Hβ emission of the nuclear zone. Spectrophotometric data of moderate resolution ($3000 < R < 11\,000$) are presented from which the physical properties of the ionized gas (electron density, oxygen abundances, ionization structure, etc.) have been derived.

1. Introduction

The inner ($\sim$1 kpc) zones of some spiral galaxies show high star formation rates frequently arranged in a ring or pseudo-ring pattern around their nuclei. In general, circumnuclear star-forming regions (CNSFRs)—also referred to as "hotspots"—and luminous and large disk H II regions are very much alike, but the former look more compact and show higher peak surface brightnesses (Kennicutt, Keel, & Blaha 1989). In many cases they contribute substantially to the emission of the entire nuclear region. Their large Hα luminosities, typically higher than $10^{39}\,\mathrm{erg\,s^{-1}}$, point to relatively massive star clusters as their ionization source. These regions, then, constitute excellent places to study how star formation proceeds in high metallicity, high density circumnuclear environments.

The importance of an accurate determination of the abundances of high metallicity H II regions cannot be overestimated since these object constitute most of the H II regions in early spiral galaxies (Sa to Sbc) and the inner regions of most late-type ones (Sc to Sd), without which our description of the metallicity distribution in galaxies cannot be complete. The question of how high the highest oxygen abundance is in the gaseous phase of galaxies is still outstanding, and the extrapolation of known radial abundance gradients would point to CNSFRs as the most probable sites for these high metallicities. Accurate measurements of elemental abundances of high metallicity regions are therefore crucial to obtaining reliable calibrations of empirical abundance estimators, widely used but poorly constrained, whose choice can severely bias results obtained for quantities of the highest relevance for the study of galactic evolution such as the luminosity–metallicity (L–Z) relation for galaxies. CNSFRs are also ideal cases for studying the behavior of abundance estimators in the high metallicity regime.

2. Observations and Measurements

We have obtained moderate-resolution observations of 12 CNSFRs in three "hot spot" galaxies (NGC 2903, NGC 3351, and NGC 3504). These three galaxies are early barred spirals and show high star formation rates in their nuclear regions. They are quoted in the literature as among the spirals with the highest overall oxygen abundances (Pérez-Olea 1996). Figure 1 shows an *HST* archive image of the circumnuclear region of one of the observed galaxies, NGC 3351, taken with the WFPC2 camera through the F606W filter.

Our observations were obtained with the ISIS double spectrograph mounted on the 4.2 m William Herschel Telescope (WHT) at the Roque de los Muchachos Observatory and provided spectrophotometry of the spectral ranges $\lambda\lambda$3650–7000 Å in the blue and $\lambda\lambda$8850–9650 Å in the near-IR, with spectral resolutions of ∼2.0 Å and 1.5 Å FWHM, respectively. Different slit positions were used to observe several distinct H II regions, as exemplified in Figure 1. The data were reduced using the IRAF (Image Reduction and Analysis Facility) package following standard procedures. The blue and red spectra corresponding to one of the observed regions are also shown in Figure 1. The presence of a conspicuous underlying stellar population in most observed regions, more evident in the blue spectra, complicates the measurements of emission lines (see the blue spectrum in Fig. 1). A two-component (emission and absorption) Gaussian fit was performed in order to correct the Balmer lines for underlying absorption.

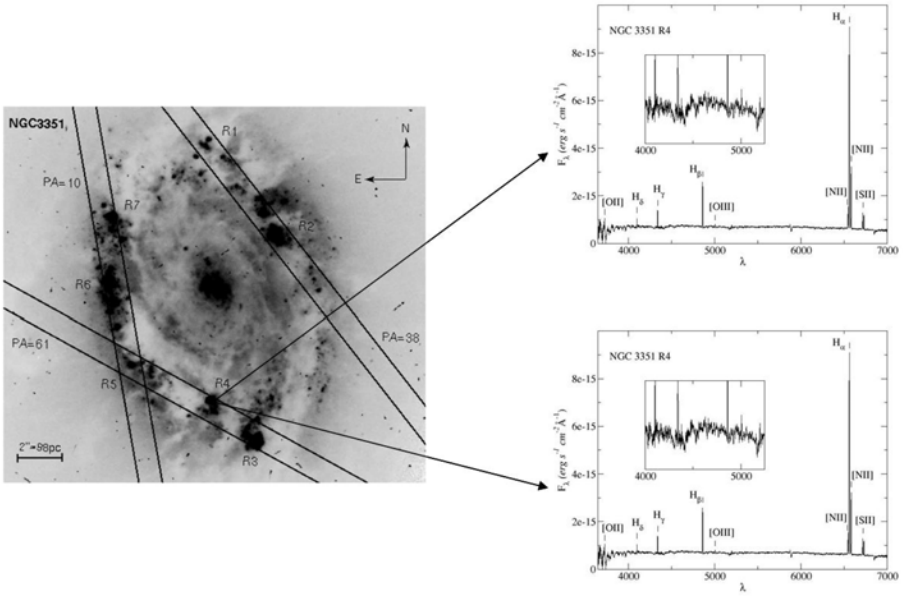

Figure 1. Observed CNSFRs in NGC 3351. The different slit positions are superimposed on an image taken from the *HST* archive and obtained with the WFPC2 camera with the F606W filter. The position angles of every slit position are indicated. The blue and red spectra corresponding to one of the observed regions are also shown.

3. Results and Discussion

Electron densities for each observed region were derived from the [S II] $\lambda\lambda$6717, 6731 Å line ratio, following standard methods. They were found to be, in all cases, $\leq 600\,\mathrm{cm}^{-3}$, higher than those usually derived in disk H II regions, but still below the critical value for collisional de-excitation. The low excitation of the regions, as evidenced by the weakness of the [O III] λ5007 Å line (see the blue spectrum in Fig. 1) precludes the detection and measurement of the auroral [O III] λ4363 Å necessary for the derivation of the electron temperature. We have therefore used a semi-empirical procedure for the derivation of abundances. Firstly, we have produced a calibration of the [S III] temperature as a function of the abundance parameter SO_{23} defined as:

$$SO_{23} = \frac{I([\mathrm{O\,II}]\lambda 3727,29) + I([\mathrm{O\,III}]\lambda 4959,5007)}{I([\mathrm{S\,II}]\lambda 6716,31) + I([\mathrm{S\,III}]\lambda 9069,9532)}.$$

This parameter is similar to the S_3O_3 proposed by Stasińska (2006) but is, in the first order, independent of geometrical (ionization parameter) effects. To perform this calibration we have compiled all the data so far available with sulfur emission line detections of both the auroral and nebular lines at λ6312 Å and $\lambda\lambda$9069, 9532 Å, respectively (see Díaz et al. 2007). The calibration is shown in Fig. 2, together with the quadratic fit to the high metallicity H II region data:

$$T_{\mathrm{e}}([\mathrm{S\,III}]) = 0.596 - 0.283 \log SO_{23} + 0.199(\log SO_{23})^2.$$

For one of the observed regions, R1+R2, the [S III] λ6312 Å line has been detected and measured yielding a value $T_{\mathrm{e}}([\mathrm{S\,III}]) = 8400^{+4650}_{-1250}$ K, represented as a solid black circle in Fig. 2 (*left*). We have used this calibration to derive $T_{\mathrm{e}}([\mathrm{S\,III}])$ for our observed CNSFRs. In all cases the values of $\log O_{23}$ are within the range used in performing the calibration, thus requiring no extrapolation of the fit. These temperatures, in turn, have been used to derive the S^+/H^+ and S^{++}/H^+ ionic ratios. Once the sulfur ionic abundances have been derived, we have estimated the corresponding oxygen abundances, assuming that sulfur and oxygen temperatures follow the relation given by Garnett (1992) and T_{e} ([O II]) $\simeq T_{\mathrm{e}}([\mathrm{S\,III}])$. Finally, we have derived the N^+/O^+ ratio assuming that $T_{\mathrm{e}}([\mathrm{O\,II}]) \simeq T_{\mathrm{e}}([\mathrm{N\,II}]) \simeq T_{\mathrm{e}}([\mathrm{S\,III}])$.

The observed CNSFRs turn out to be of high metallicity, but they show marked differences with respect to high metallicity disk H II regions. Even though their derived oxygen and sulfur abundances are similar, they show values of the O_{23} and the N2 parameters whose distributions are shifted to lower and higher values, respectively, with respect to the high metallicity disk sample. Hence, if purely empirical methods were used to estimate the oxygen abundances for these regions, higher values would in principle be obtained. This would seem to be in agreement with the fact that CNSFRs, when compared to the disk high metallicity regions, show the highest [N II]/[O II] ratios.

CNSFRs also show lower ionization parameters than their disk counterparts, as derived from the [S II]/[S III] ratio. Their ionization structure also seems to be different, with CNSFRs showing radiation field properties more similar to those of H II galaxies than to those of disk high metallicity H II regions. This can be

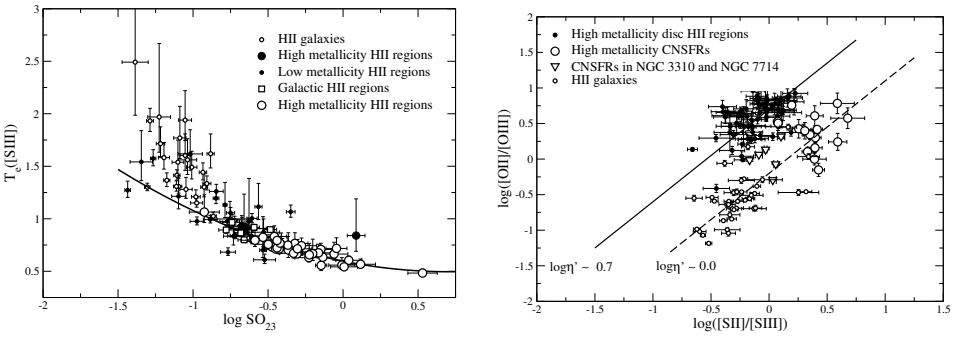

Figure 2. *Left:* Empirical calibration of the [S III] electron temperature as a function of the abundance parameter SO_{23}. The solid line represents a quadratic fit to the high metallicity H II region data. *Right:* The [O II]/[O III] vs [S II]/[S III] logarithmic ratios for different ionized regions. References for the data in the two figures can be found in Díaz et al. (2007).

seen in Fig. 2 (*right*), a diagram of the [O II]/[O III] vs [S II]/[S III] emission line ratios, that works as a diagnostic for the nature and temperature of the radiation field. In this plot, diagonal lines of slope unity show the locus of ionized regions with constant ionization temperature. CNSFRs are seen to segregate from disk H II regions. The former cluster around a value of $T_{\rm ion} \sim 40\,000$ K, while the latter cluster around $T_{\rm ion} \sim 35\,000$ K. Also shown are the data corresponding to H II galaxies. Indeed, CNSFRs seem to share more the locus of H II galaxies than that of disk H II regions.

One possible concern about these CNSFRs is that, given their proximity to the galactic nuclei, they could be affected by hard radiation coming from a low luminosity AGN. Alternatively, the spectra of these regions harboring massive clusters of young stars might be affected by the presence of shocked gas. Diagnostic diagrams of the kind presented by Baldwin, Phillips, & Terlevich (1981) can be used to investigate the possible contribution by either a hidden AGN or the presence of shocks to the emission line spectra of the observed CNSFR. When plotted on one of these diagnostic diagrams, $\log([\mathrm{N\,II}]/\mathrm{H}\alpha)$ vs $\log([\mathrm{O\,III}])/\mathrm{H}\beta$, some of our CNSFRs are found close to the transition zone between H II region and LINER spectra but only one region in NGC 3504 may show a hint of a slight contamination by shocks.

Acknowledgments. We acknowledge financial support from DGICYT grant AYA-2004-02860-C03. AID thanks the hospitality of the Institute of Astronomy, Cambridge, during her sabbatical financed by the Spanish MEC through grant PR2006-0049.

References

Baldwin, J. A., Phillips, M. M., & Terlevich, R. 1981, PASP, 93, 5
Díaz, A. I., Terlevich, E., Castellanos, M., & Hägele, G. F. 2007, MNRAS, submitted
Garnett, D. R. 1992, AJ, 103, 1330
Kennicutt, R. C., Keel, W. C., & Blaha, C. A. 1989, AJ, 97, 1022
Pérez-Olea, D. 1996, PhD Thesis, Univ. Autónoma de Madrid

Stasińska, G. 2006, A&A, 454, L127

Discussion

Pagel: The circumnuclear H II regions presumably occupy a peculiar position in, for example, [O III] vs [N II] diagrams.

Díaz: These regions actually show two kinematic components in the ionized gas, both in H I and [O III], the wider of which shows a velocity dispersion which agrees with that shown by stellar lines. If that is taken into account, the gas with the wider component shows [O III]/Hβ higher than that shown by the gas with the narrow component. But I can say nothing about the [N II]/Hα ratio since we do not have comparable high resolution data for these lines. At any rate, everything points to these CNSFRs being in the low excitation region in the diagnostic diagram and not in the zone occupied by LINER-like objects.

Ercolano: The fact that abundance indicators for high metallicity overestimate the abundances may be due to geometrical effects of the spatial distribution of stars (see B. Ercolano, N. Bastian, & G. Stasińska [2007, MNRAS, 379, 945] and the poster, this volume, p. 110).

Díaz: If this is the case, then since CNSFRs show average values of abundance calibrators different from disk high metallicity regions, this would indicate different spatial distributions for these two types of star-forming regions. Semi-empirical abundance derivation should then be considered as more reliable. This would lead us to conclude that it is very difficult to find oxygen abundance higher than solar. Also, one has to explain the high N/O ratios in CNSFRs, by up to five times solar.

Ángeles Díaz.